Available online at www.sciencedirect.com

ScienceDirect

journal homepage: www.elsevier.com/locate/he

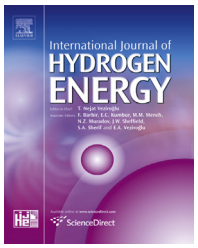

Study of the performance of $Rh/La_2O_3–SiO_2$ and Rh/CeO_2 catalysts for SR of ethanol in a conventional fixed-bed reactor and a membrane reactor

Adriana M. da Silva [a], *Lisiane V. Mattos* [b], *John Múnera* [c], *Eduardo Lombardo* [c], *Fabio B. Noronha* [a], *Laura Cornaglia* [c,*]

[a] *Instituto Nacional de Tecnologia, Av. Venezuela 82, Rio de Janeiro, 20081-312, Brazil*
[b] *Universidade Federal Fluminense, Rua Passo da Pátria 156, Niterói, 24210-240, Brazil*
[c] *Instituto de Investigaciones en Catálisis y Petroquímica, INCAPE (FIQ, UNL-CONICET), Santiago del Estero 2829, 3000, Santa Fe, Argentina*

ARTICLE INFO

Article history:
Received 4 September 2014
Received in revised form
30 December 2014
Accepted 19 January 2015
Available online 19 February 2015

Keywords:
Ethanol steam reforming
Rh-based catalysts
Membrane reactor

ABSTRACT

The performance of $Rh/La_2O_3–SiO_2$ and Rh/CeO_2 catalysts for steam reforming of ethanol was investigated in a conventional fixed-bed reactor and a membrane reactor. This reactor was built with a self-supported Pd–Ag membrane, and its performance was compared to that the conventional reactor employing the same residence time and temperature. The effect of steam to ethanol molar ratio, ethanol concentration, temperature and contact time over hydrogen permeation and hydrogen recovery was investigated. In all cases, the ethanol conversion was kept at 100%, and the products formed were only H_2, CO_2, CO and CH_4. In the membrane reactor, the overall ethanol reforming reaction was favored without the formation of carbon deposits. The highest permeated and H_2 recovery was obtained for low ethanol content in the feed (high H_2O/Ethanol ratio) and the methane formation was unfavored, in agreement with the high production of hydrogen.

A slight difference in the hydrogen permeated/feed ethanol ratio was observed at higher sweep gas flow rates being higher for Rh supported on CeO_2 in comparison with the $Rh/La_2O_3–SiO_2$ catalyst. The best results were obtained with a H_2O/Ethanol molar ratio equal to 10 and the highest membrane permeation area. Under these conditions, the H_2 recovery reached values of about 70% and the hydrogen produced for each mole of ethanol exhibited the highest value close to 2.8.

Introduction

Proton exchange membrane (PEM) fuel cells are an alternative for clean power generation. However, they require highly pure hydrogen as the cell electrodes are poisoned by even small amounts of CO [1]. Different approaches have been widely used to accomplish such a goal, involving integrated reaction units for CO clean-up such as: water-gas shift; CO selective oxidation; methanation [2]. Hydrogen-selective and -permeable Pd

* *Corresponding author.*
E-mail address: lmcornag@fiq.unl.edu.ar (L. Cornaglia).
http://dx.doi.org/10.1016/j.ijhydene.2015.01.106

membranes are a promising technology for the production of H_2 with high purity. The use of membrane reactors for the production of CO-free hydrogen has many advantages: (i) production and purification can be achieved in the same equipment, which results in the reduction of hydrogen costs; (ii) the thermodynamic equilibrium can be overcome by the continuous hydrogen removal from the reaction zone [3].

Different types of membranes have recently been applied in membrane reactor (MR) for different reactions [3]. The reactor performance is highly dependent on the conditions under which the reactions are carried out, such as membrane permeance, membrane selectivity, space velocity, temperature and reactor pressure, concentration and nature of reactants [4]. In a recent study, we investigated the performance of a double tubular MR built with a commercial self-supported Pd–Ag membrane or with a composite Pd membrane supported on porous stainless steel [5]. Both membrane reactors were tested for the production of hydrogen through the carbon dioxide reforming of methane with and without oxygen addition. The composite Pd membrane reactor exhibited a higher H_2 permeated/CH_4 fed ratio increase with the sweep gas flow rate at 450 °C, which could be related to its higher hydrogen permeability. To perform a better comparison between the best catalysts applied in the membrane reactors (Rh and Ru supported on La_2O_3–SiO_2 or on lanthanum oxycarbonate), the H_2 permeated/CH_4 fed ratio expressed by permeation area (mol s^{-1} m^{-2}) was analyzed for self-supported PdAg membrane reactors operated at 550 °C [5,6]. These values show that the Ru/$La_2O_2CO_3$ and the Rh/La_2O_3–SiO_2 solids displayed ratios higher than those observed for Ru/La_2O_3–SiO_2, when the dry reforming of methane was carried out. Carbon deposition was not detected for all catalysts.

Different feedstocks have been used for the production of hydrogen such as biomass and its derived liquids. As a consequence, it does not contribute to CO_2 emissions due to the well-known carbon cycle. The steam reforming (SR) of ethanol has been extensively studied for the production of hydrogen [7–9]. Ethanol is non-toxic, easy to handle and the infra-structure for production and distribution is already established in some countries like the United States and Brazil, which is adequate for the decentralized production of hydrogen.

In the case of ethanol conversion reactions, a recent review examined the benefits and the main drawbacks of inorganic membrane reactors, paying particular attention to the effect of the different typologies of inorganic membranes on the reaction performance in terms of hydrogen yield, hydrogen recovery and ethanol conversion [10]. In addition, the MR parameters were qualitatively compared to those of conventional reactors. The first studies of the SR of ethanol in membrane reactors were related to the simulation and modeling of the process [10–14]. In the last four years, the number of experimental studies using membrane reactors for the SR of ethanol have increased [15–24]. Tosti et al. [15] carried out a kinetic study of the SR of ethanol over Ru, Pt, and Ni based catalysts in a Pd–Ag membrane and analyzed the results using a power-rate law model. Non-commercial Pd–Ag tubes of thin wall (50–60 μm) have been produced at their laboratories via a cold-rolling. These wall tubes were applied to membrane reformers and exhibited the capability to produce ultra pure hydrogen with high reaction conversions.

Recently, Oyama and coworkers [22,25] carried out a study of the SR of ethanol over a Co–Na/ZnO catalyst both in a packed-bed reactor (PBR) and MRs equipped with ultrathin Pd or Pd–Cu membranes, and with a silica–alumina composite membrane with different H_2 permeability and selectivity. In all studies, ethanol conversion and hydrogen yield in the MRs were significantly higher than in the PBR. However, a significant contamination of the Pd layer by CO or carbon compounds during the reaction was observed. The hydrogen permeation properties decreases due to the penetration of the carbon atoms and expansion of Pd lattice, leading to membrane failure [25].

Carbon formation is still a challenge during ethanol conversion reactions carried out in conventional reactors as well as in membrane reactors [7]. Different strategies have been proposed to minimize or inhibit carbon formation such as the modification of the catalyst support. The nature of the support can strongly influence the stability of the catalyst during SR of ethanol by assisting in the removal of carbon or suppressing its formation [7,26–28]. The addition of La_2O_3 to a Ni/Al_2O_3 catalyst significantly decreased the rate of carbon deposition due to the coverage of the acidic sites of alumina by the basic lanthana species. These acid sites could be responsible for the dehydration reaction. Fatsikostas et al. [28] proposed that the LaO_x species formed during reduction could react with CO_2 to produce $La_2O_2CO_3$. This lanthanum oxycarbonate species can react with carbon to form CO and regenerate La_2O_3 by promoting the removal of carbon. Redox supports such as ceria and ceria-containing mixed oxides improve catalyst stability due to their high oxygen storage capacity (OSC) and oxygen mobility [7]. This highly mobile oxygen can react with carbon species formed during the reaction and thus keeps the metal surface free of carbon, inhibiting deactivation. Recently, we demonstrated that Rh/CeO_2 catalyst is quite stable under SR of ethanol carried out in a fixed-bed reactor [29]. This high stability of this catalyst was attributed to a greater fugacity of available O from the support to assist in removing carbonaceous species.

Therefore, the goal of this work was to study the performance of Rh-based catalysts for the SR of ethanol using a self-supported commercial Pd–Ag membrane reactor. Two different catalyst supports were employed: CeO_2 and La_2O_3/SiO_2. Previous results of our groups showed that these supports inhibited carbon formation for reactions in which this is expected. The effect of steam to ethanol molar ratio, ethanol concentration, temperature, contact time and sweep gas flow rate over hydrogen permeation and hydrogen recovery was investigated. In addition, the performance of the membrane reactor was compared to that the conventional reactor employing the same residence time and temperature.

Experimental

Catalyst preparation

La_2O_3–SiO_2 support was prepared by the incipient wetness impregnation of SiO_2 (Aerosil 200, calcined at 1173 K) with lanthanum nitrate (Aldrich 99.9%) in order to obtain 27 wt.% of La_2O_3. The support was calcined for 6 h at 823 K in flowing air.

The metal deposition was performed by the incipient wetness impregnation of the support by using $RhCl_3.3H_2O$ (Alfa Aesar). Then, the sample was dried at 393 K overnight, followed by calcination in air at 823 K for 6 h. The nominal Rh loading was 0.6 wt. % for this catalyst.

CeO_2 support with a high surface area was prepared. At first, an aqueous solution containing the precursor cerium (IV) ammonium nitrate (Acros) was prepared. Then, an aqueous solution of ammonium hydroxide was slowly added to the cerium aqueous solution for precipitation. Afterwards, the temperature was raised up to 366 K and the system was held under these conditions for 96 h. The pH of the solution containing the precipitate was maintained at 10 during that time. The precipitate was collected by centrifugation and the material was washed until a pH of 7 was reached. Then, the sample was dried at 393 K for 12 h and calcined in a muffle furnace at 773 K for 12 h. Rh was added to CeO_2 support by incipient wetness impregnation using an aqueous solution of $RhCl_3.3H_2O$ (Aldrich). The nominal Rh content was 1 wt%. After impregnation the samples were dried at 393 K for 12 h and calcined in air at 673 K for 2 h.

Catalyst characterization

Surface area

The BET (Brunauer, Emmett, and Teller) surface area was determined from N_2 adsorption isotherms at liquid nitrogen temperature using a Quantachrome Autosorb automatic gas adsorption instrument. Prior to the measurements, all samples were degassed at 423 K under a 0.13 Pa overnight.

Metal dispersion

For the $Rh/La_2O_3{-}SiO_2$ catalyst, the metal dispersion of the fresh catalyst was determined by the static equilibrium adsorption of either H_2 at 373 K or CO at 298 K in a conventional vacuum system, following the hydrogen reduction at 823 K for 1 h. Since H_2 and CO adsorption may occur over CeO_2 support, Rh dispersion could not be determined from chemisorption of both gases for the Rh/CeO_2 catalyst. In this case, the metal particle size was determined using HR-TEM and STEM. Electron microscopy studies were performed using a JEOL 2010F STEM outfitted with a URP pole piece, GATAN 2000 GIF, GATAN DigiScan II, Fischione HAADF STEM detector, and EmiSpec EsVision software. The catalyst was reduced at 773 K for 1 h, cooled to room temperature under helium and then passivated with a mixture containing 1% O_2/He.

Laser Raman Spectroscopy (Raman)

The Raman spectra were recorded using a LabRam spectrometer (Horiba-Jobin-Yvon) coupled to an Olympus confocal microscope (a 100× objective lens was used for simultaneous illumination and collection), equipped with a CCD detector cooled to about 200 K using the Peltier effect. The excitation wavelength was in all cases 532 nm (Diode-pumped solid-state laser). The laser power was set at 30 mW.

X-ray photoelectron spectroscopy (XPS)

The XPS measurements were carried out using a multitechnique system (SPECS) equipped with a dual Mg/Al X-ray source and a hemispherical PHOIBOS 150 analyzer operating in the fixed analyzer transmission (FAT) mode. The spectra were obtained with a pass energy of 30 eV; the Mg Kα X-ray source was operated at 200 W and 12 kV. The working pressure in the analyzing chamber was less than 6×10^{-7} Pa.

Prior to the XPS analyses, the solids were reduced in flowing hydrogen in a fixed-bed reactor at 823 K for 2 h. After that, they were exposed to a steam flow (7.5% water in Ar) at the same temperature during 12 h. The data were processed with the Casa XPS program (Casa Software Ltd., UK). The peak areas were determined by integration employing a Shirley-type background. Peaks were considered to be a mix of Gaussian and Lorentzian functions in a 70/30 ratio. For the quantification of the elements, sensitivity factors provided by the manufacturer were used.

Catalytic test

Conventional fixed-bed reactor (CR)

Ethanol steam reforming was performed in a quartz reactor at atmospheric pressure. A small amount of catalyst (20 mg) was used in order to study the catalyst deactivation within a short period of time. The samples were diluted with inert SiC (SiC mass/catalyst mass of 3.0). Before the catalytic tests, the samples were reduced *in situ* under H_2 at 773 K for 1 h and then purged under N_2 at the same temperature for 30 min. All reactions were performed at 773 K using an ethanol/H_2O molar ratio of 3.0. The reactant mixture (2.5% ethanol; 7.5% water, 90.0% nitrogen) was obtained by flowing two N_2 streams (30 mL/min) through each saturator containing ethanol and water separately.

Membrane reactor (MR)

The double tubular membrane reactor was built using a commercial self-supported tubular Pd–Ag membrane with a thickness of 75 μm, provided by R&B Research and Consulting, with one end closed and an inner tube to allow N_2 sweep gas (SG) flow. The difference in the hydrogen partial pressure between the reaction and permeation sides was the driving force for H_2 permeation. The rate of hydrogen permeation was enhanced by the sweeping gas flow rate [4,5,30]. The outer tube was made of commercial non-porous quartz (i.d. 9 mm). The catalyst (20 mg), diluted with quartz chips to obtain a bed height of 2.5 or 4 cm, was packed in the outer annular region (shell side) (Fig. 1). The permeation area was 2.5 or 4×10^{-4} m^2, respectively. Both sides of the membrane were kept at atmospheric pressure in all runs. The catalysts were heated under N_2 flow to 773 K and then reduced *in situ* under a H_2 stream at the same temperature for 1 h. Subsequently, the reaction mixture containing water and ethanol was fed to the reactor as described for the conventional fixed-bed reactor. The reactions were performed at 773 K or 823 K using three different ethanol/H_2O molar ratios of 3.0, 6.0 and 10.0. The ethanol flow rate was kept constant in all experiments. The reactions were also carried out at two different W/Q, 0.028 g s/mL and 0.056 g s/mL.

The permeability of similar REB commercial membranes has been reported elsewhere [5]. At the reaction temperatures, the permeability was equal to 5.6×10^{-9} and 7.1×10^{-9} mol m^{-1} s^{-1} $Pa^{-0.5}$ at 773 and 823 K, respectively.

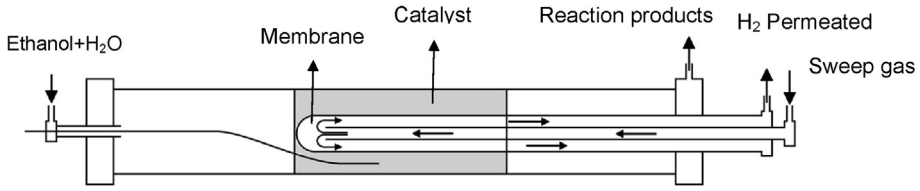

Fig. 1 – Membrane reactor scheme.

The constancy of the permeation characteristics was checked after the MR runs. Only hydrogen was detected in the permeate stream in all cases, consistent with the infinite selectivity of the membrane.

The reaction products from both the conventional fixed-bed and the membrane reactors were analyzed by gas chromatography (Micro GC Agilent 3000 A) containing three channels with thermal conductivity detectors (TCD) and three columns: a molecular sieve, a plot Q and a OV-1 column. Ethanol conversion, products distribution and hydrogen recovery were determined from:

$$X_{ethanol} = \frac{(n_{ethanol})_{fed} - (n_{ethanol})_{exit}}{(n_{ethanol})_{fed}} \times 100 \quad (1)$$

$$S_x = \frac{(n_x)_{produced}}{(n_{total})_{produced}} \times 100 \quad (2)$$

$$H_2 recovery(\%) = \frac{H_2 permeated}{H_2 produced} \times 100 \quad (3)$$

where (n_x)produced = moles of x produced (x = hydrogen, CO, CO_2, methane, acetaldehyde or ethene) and (n_{total}) produced = moles of H_2 + moles of CO + moles of CO_2 + moles of acetaldehyde + moles of ethene (the moles of water produced are not included).

Results and discussion

Rh particle size measurements

To determine the metal particle size of both catalysts, CO chemisorption, HRTEM and XPS measurements were carried out. For the $Rh/La_2O_3–SiO_2$ catalyst, the Rh dispersion measured by CO chemisorption was 79%, which corresponds to a Rh particle size of 1.4 nm. In the case of the Rh/CeO_2 catalyst, the metal particle size was determined by HRTEM/STEM. The value varied from 4 to 8 nm, denoting that the Rh particles were almost the same size. Moreover, the metallic dispersion calculated for this catalyst was around 38.8% assuming that the Rh particles were spherical [29]. In order to investigate the modification of the metal particle size with the reaction temperature and in the presence of the reactants, the catalysts were characterized by XPS after reduction at 823 K followed by a treatment in a steam flow at the same temperature. These results are summarized in Table 1. Regarding the binding energy (BE) of the Rh $3d_{5/2}$ peak, the low binding energies of reduced samples indicates the reduction to Rh^0 in both solids. The FWHM (Full width at High Maximum) of the Rh $3d_{5/2}$ peak mainly reflects the particle size [31]. The increased FWHM for small particles, where the BE is also sensitively size dependent, originates from the particle size distribution. The $Rh/La_2O_3–SiO_2$ catalyst exhibits larger FWHM as well as BE than the reduced Rh/CeO_2 catalyst. This indicates smaller average particle size and broader size distribution in the $Rh/La_2O_3–SiO_2$ catalyst, in agreement with the high metal dispersion (79%). For this catalyst, the Rh/(La + Si + O) atomic ratio is lower in the reduced than in the exposed-to-steam sample, suggesting that a variation in the rhodium dispersion occurred during this treatment. However, no significant modification in the Rh binding energy assigned to Rh^0 and in the FWHM was observed (Fig. 2a).

In the case of the Rh/CeO_2 catalyst, the appearance of a shoulder in the high BE side of the Rh $3d_{5/2}$ peak was observed after the steam treatment, indicating the presence of a second peak, assigned to Rh^{+n} species (Fig. 2b). In addition, the $Ce_{916.5}/Ce_{total}$ ratio increased from 0.05 in the reduced catalysts to 0.12, suggesting the surface re-oxidation of Ce^{+3} to Ce^{+4}. Note that the O/Ce ratio also increased. However, the surface Rh/(Ce + O) ratio did not change in the sample exposed to a steam flow.

Fig. 3 compares the Ce 3d spectra for the reduced (a) and treated with H_2O vapor (b) Rh/CeO_2 catalyst. In a reference CeO_2 sample, six peaks, V1, V2, V3, U1, U2, and U3, corresponding to three pairs of spin–orbit doublets, were identified in the Ce 3d spectrum (Fig. 3c). For this reference, the area of the highest binding energy peak (U3 at 916.5 eV) in the Ce 3d region, relative to the area of the entire Ce 3d region was close to 12.7%.

Shyu et al. [32] proposed that this ratio determines the relative amounts of Ce^{+3} and Ce^{+4} in a given sample. The 12% value indicates a fully oxidized cerium dioxide (Ce^{+4}). This analysis was previously applied to catalysts supported on cerium oxides and mixed oxides [33–35].

In the reduced Rh/CeO_2 catalysts, the intensity of the U3 peak significantly decreased and new peaks appears, which were assigned to two pairs of spin–orbit doublets (V0,V, U0 and U peaks). This indicates that Ce $^{+4}$ changed into Ce $^{+3}$ by releasing lattice oxygen. The relative intensity of the U3 peak shows a value of 5% for the reduced sample (Table 1), indicating that 60% of surface Ce is present as Ce^{+3}. However, when this catalyst is treated with steam, a strong surface Ce re-oxidation occurs and only 6% of surface Ce remains as to $Ce^{+3.}$

Steam reforming of ethanol in a conventional fixed-bed reactor (CR)

The ethanol conversion and product distributions as a function of time-on-stream (TOS) for steam reforming of ethanol

Table 1 – Binding energies and surface atomic ratios of reduced solids and after steam treatment in a fixed-bed reactor at 823 K.

Samples	Treatment	Rh $3d_{5/2}$ (eV)	Rh/M + O	O/M[a]	Si/La	Ce_{U3}/Ce_{total}[b]	% Ce^{+3}[c]
$Rh/La_2O_3–SiO_2$	Reduced	307.2 (3.4)[d]	0.0017	1.8	7.3	–	
	Steam	307.7 (3.6)	0.001	1.9	11	–	
Rh/CeO_2	Reduced	306.8 (2.0)	0.008	2.5	–	0.05	61
	Steam	306.6 (72%)[e] (2.0) 308.3 (28%) (2.0)	0.0075	4.3	–	0.12	6

[a] M corresponds to Ce or La + Si.
[b] U3 peak area relative to the area of the entire Ce 3d region.
[c] % Ce^{+3} calculated considering a relative intensity of 12.7% for CeO_2 (Ce^{+4}).
[d] FWHM (eV) are given between parenthesis.
[e] Relative % of Rh species.

over $Rh/La_2O_3–SiO_2$ and Rh/CeO_2 catalysts are depicted in Fig. 4A and B, respectively. Both catalysts exhibited high activity (100% of ethanol conversion) and they were quite stable, even after 28 h TOS. Moreover, the product distribution obtained was quite similar for both catalysts. The main products formed were H_2, CO_2, CO and CH_4, indicating that steam reforming and water-gas shift were the main reactions taking place. The ethanol conversion was measured in an empty fixed bed reactor showing values close to 10% [36].

The catalysts used in the SR of ethanol were characterized by Raman Spectroscopy in order to evaluate the formation of carbon. The Rh/CeO_2 and $Rh/La_2O_3–SiO_2$ catalysts did not show any bands related to carbonaceous species. These results explain the high activity of these catalysts during the ethanol steam reforming reaction.

The stability exhibited by the Rh/CeO_2 catalyst for the SR of ethanol is quite unusual mainly because it was used a low H_2O/ethanol molar ratio. The outstanding performance could be associated with the high Oxygen Storage Capacity (OSC) of the support, which promotes the carbon removal. Furthermore, the small Rh particles (4–5 nm) measured by HRTEM would assist in the catalyst stability since the carbon deposit is expected to occur at large metallic ensembles [29].

Concerning the $Rh/La_2O_3–SiO_2$ catalyst, a high resistance to carbon deposition was also observed during the SR of ethanol. A similar mechanism would be expected but with some differences related to the support nature. As a matter of fact, Fatsikostas and Verykios [28] showed that the impregnation of Al_2O_3 with La_2O_3 led to an improvement on the stability of the catalyst $Ni/La_2O_3–Al_2O_3$ during ethanol steam

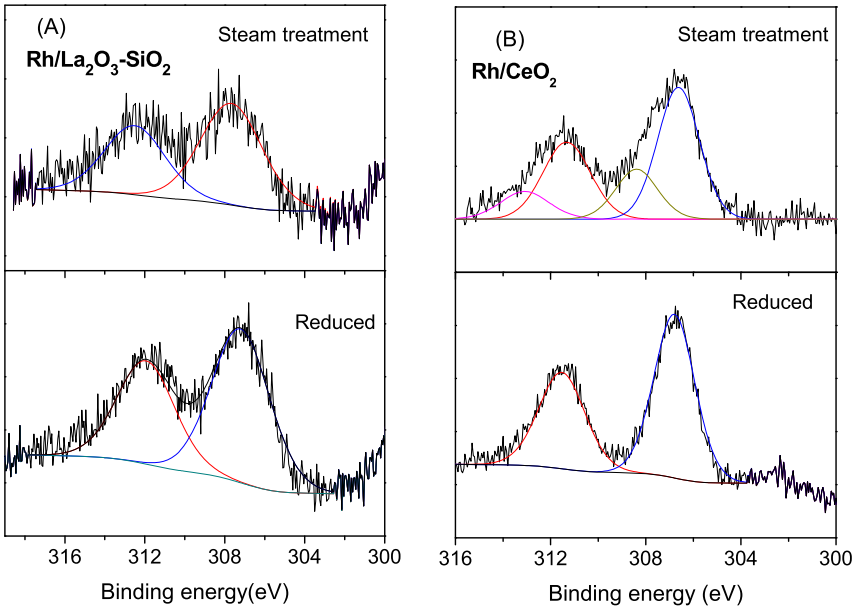

Fig. 2 – XP spectra for the Rh 3d region of the reduced and treated with H_2O vapor Rh catalysts. (A) $Rh/La_2O_3–SiO_2$ and (B) Rh/CeO_2.

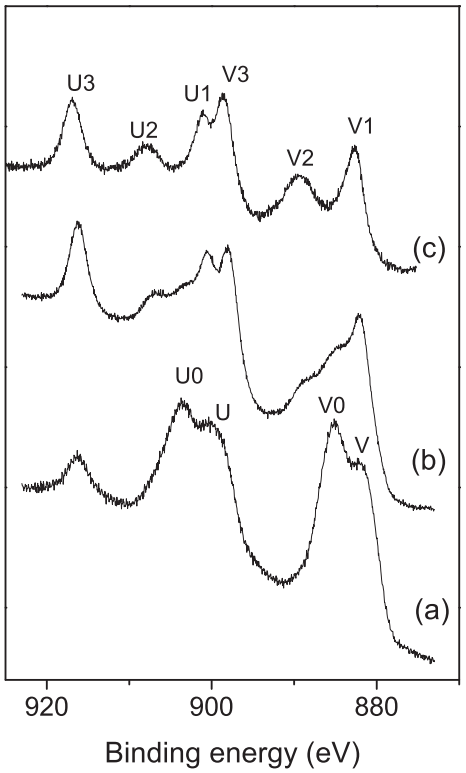

Fig. 3 – XP spectra for the Ce 3d region of the reduced (a) treated with H_2O vapor (b) Rh/CeO_2 catalyst and a reference CeO_2 sample (c).

reforming. According to these authors, lanthanum oxide species (LaO_x) tend to migrate to the Ni particle and react with carbon dioxide under reaction conditions generating lanthanum oxycarbonate species, $La_2O_2CO_3$. The stability was attributed to a reaction between lanthanum carbonate with carbon leading to La_2O_3 and CO.

In the case of Rh supported on La_2O_3–SiO_2, we have previously published [37] that the amount of oxycarbonate produced during the dry reforming of methane is low, mainly due to the presence of lanthanum disilicate. As a consequence, the availability of La_2O_3 to form the oxycarbonates is limited and they could only be formed at surface level. The high stability of the La_2O_3–SiO_2 catalysts was assigned to the formation of amorphous lanthanum disilicate, which led to an appropriate interaction between Rh and lanthanum with influence on metal dispersion.

In the case of ethanol steam reforming, a catalyst with lower La_2O_3 content (15 wt.%) exhibited larger particle size as well as higher stability after SR of ethanol for 25 h [38]. The high stability of the catalyst was assigned to the interaction between Rh and lanthanum which leads into low dispersion (particle sizes close to 3 nm) that inhibits the Rh oxidation under reaction conditions.

Since Rh/La_2O_3–SiO_2 and Rh/CeO_2 catalysts were stable during SR of ethanol with no carbon formation, the same reaction conditions were selected to operate the membrane reactor. In this case, the ethanol conversion was always kept at 100%, and the products formed were only H_2, CO_2, CO and CH_4. While the stability results are very promising is important to note that for considering the scaling up of this technology, tests that include several start-ups and shutdowns of the reaction system are necessary.

Steam reforming of ethanol in a MR

To evaluate the advantage of using a MR for the production of ultrapure hydrogen, a self-supported commercial Pd–Ag membrane was incorporated to the reactor. As it is well known, when a MR is used, the effect of several operation variables over the reactant conversion, hydrogen permeation and hydrogen recovery (defined as the ratio of the H_2 permeated and the total H_2 produced) should be considered. The first studies of the SR of ethanol in membrane reactors were related to the simulation and modeling of the process [10–14].

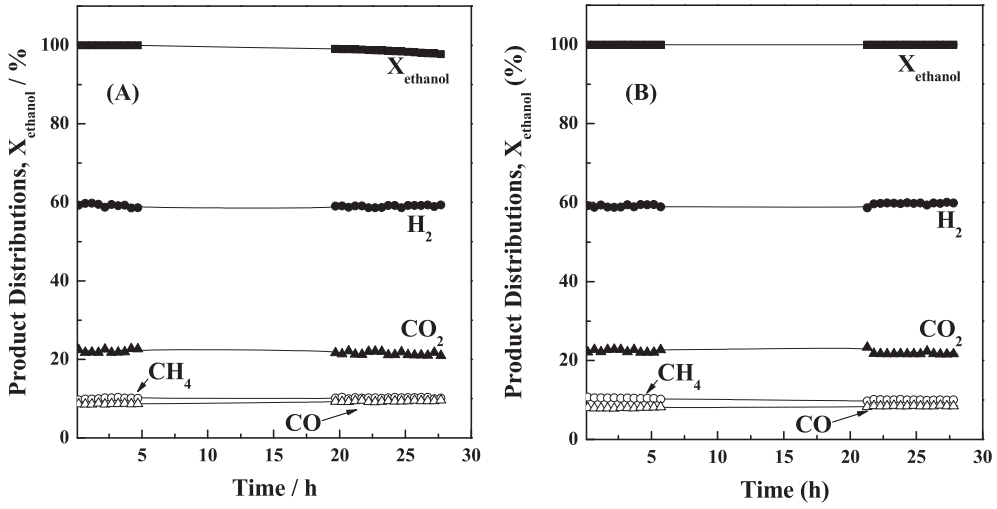

Fig. 4 – Stability tests for (A) Rh/La_2O_3–SiO_2 and (B) Rh/CeO_2, W/Q = 0.02 g s/mL, Conventional fixed-bed reactor. Reaction Conditions: T = 773 K, H_2O/ethanol = 3.0, Ethanol composition = 2.5%.

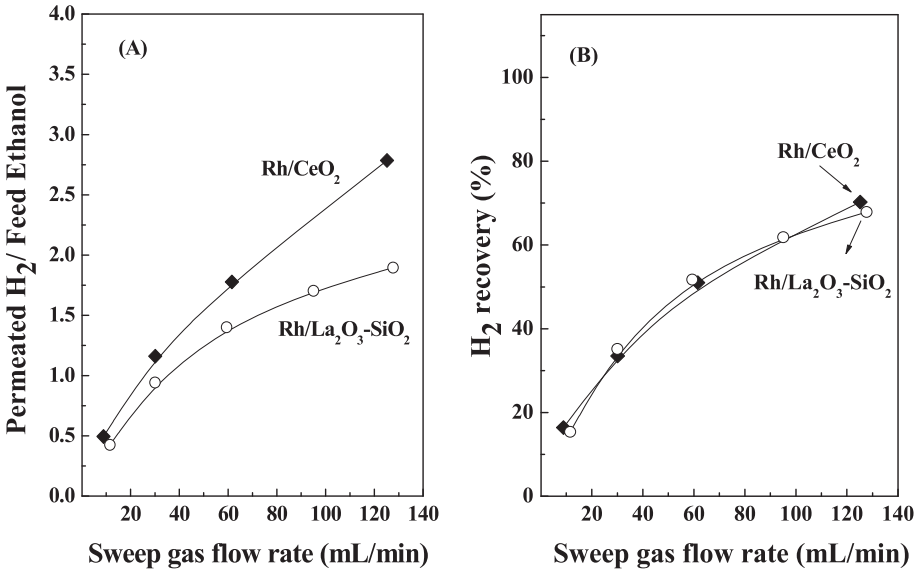

Fig. 5 – Comparison of the catalyst behavior in the membrane reactor. (A) H_2 permeated/ethanol fed ratio and (B) H_2 recovery. Reaction Conditions: T = 823 K, H_2O/ethanol = 10.0, Ethanol composition = 2.5%, W/Q = 0.028 g s/mL, Permeation area: 4.0 × 10^{-4} m^2.

However, in recent years the number of articles focused on experimental measurements has increased [15–23,39]. In the present work, a set of parameters influencing the reactor performance was studied, employing catalysts that avoid carbon formation in the applied operating conditions. In all cases, the ethanol conversion was close to 100% to keep away from the formation of by-products that could favor coke deposition. The contamination of the Pd alloy membrane by carbon deposits could lead to membrane failure.

Two different permeation areas were employed; the effect of the H_2O/Ethanol ratio, the comparison between both reactor types and the effect of temperature was investigated employing a permeation area equal to 2.5 × 10^{-4} m^2. To increase, both the H_2 permeated/ethanol fed ratio and H_2 recovery, a higher permeation area was used (4 × 10^{-4} m^2). This value was selected to analyze the effect of ethanol composition, W/Q and the catalyst comparison.

Comparison between Rh-based catalysts

When a hydrogen selective Pd membrane is used, an important issue to be considered is the catalytic system. A catalyst that exhibits high activity and stability for SR of ethanol with high resistance to coke formation is required. Note that both catalysts studied in this work comply with these requirements (Fig. 4). The comparison of H_2 permeated and H_2 recovery for Rh/La_2O_3–SiO_2 and Rh/CeO_2 catalysts in the MR with a permeation area of

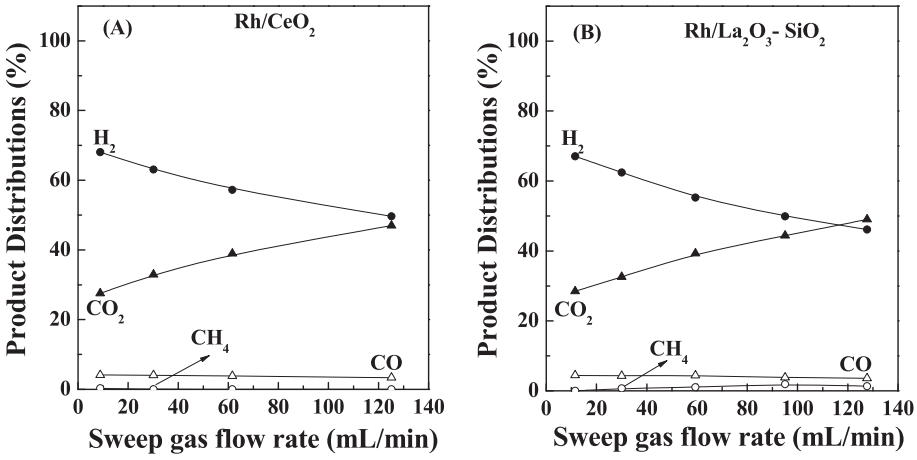

Fig. 6 – Product distribution for A) Rh/CeO_2 and B) Rh/La_2O_3–SiO_2 in a membrane reactor. Reaction Conditions: T = 823 K, H_2O/ethanol = 10.0, Ethanol composition = 2.5%, W/Q = 0.028 g s/mL, Permeation area: 4.0 × 10^{-4} m^2.

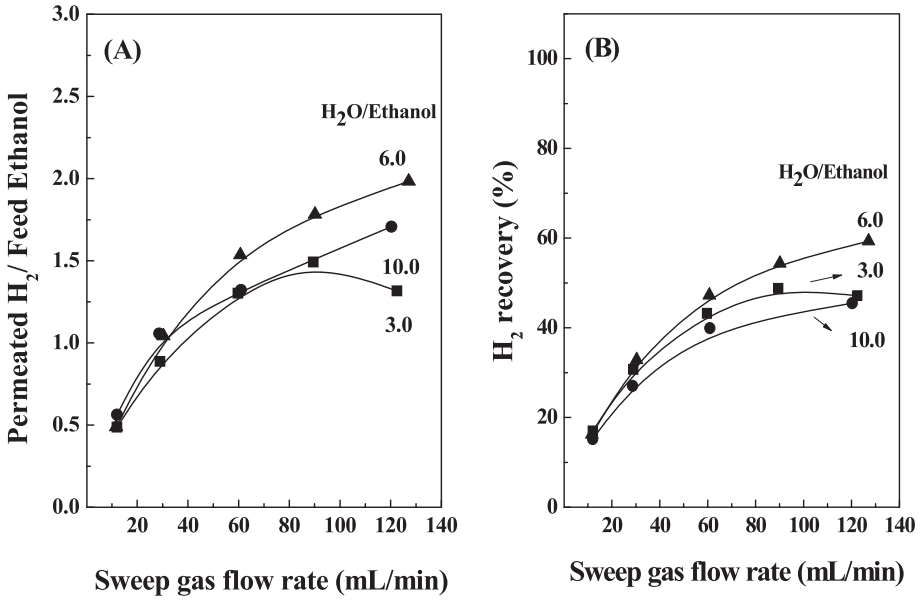

Fig. 7 – Effect of the H_2O/Ethanol ratio on the H_2 permeated/ethanol fed ratio (A) and H_2 recovery (B). Catalyst: Rh/CeO_2. Reaction Conditions: T = 773 K, Ethanol composition = 2.5%, W/Q = 0.028 g s/mL, Permeation area: 2.5×10^{-4} m^2.

4×10^{-2} m^2 at 823 K is shown in Fig. 5. Under these conditions, the H_2 recovery reached values about 70% with the additional advantage of producing high purity hydrogen.

Regarding the permeated hydrogen/feed ethanol ratio, a slight difference was observed between both catalysts at low SG flow rates. This difference increases by increasing the SG flow rate, which could be related to the difference in hydrogen yield of both systems. The product distribution as a function of the SG flow rates is shown in Fig. 6. It is observed that there is a slight difference in the hydrogen selectivity at higher SG flow rates, being higher for Rh supported on CeO_2. For the $Rh/La_2O_3–SiO_2$ catalyst, the concentration of H_2 is lower and the methane concentration slightly increases with the sweep gas flow rate. This is because this catalyst tends to produce more CH_4, lowering the hydrogen produced in the reaction side. In addition, for both catalysts, the CO formation remained constant in all range of SG flow rate studied (Fig. 6). Additionally, no formation of oxygenated compounds was observed.

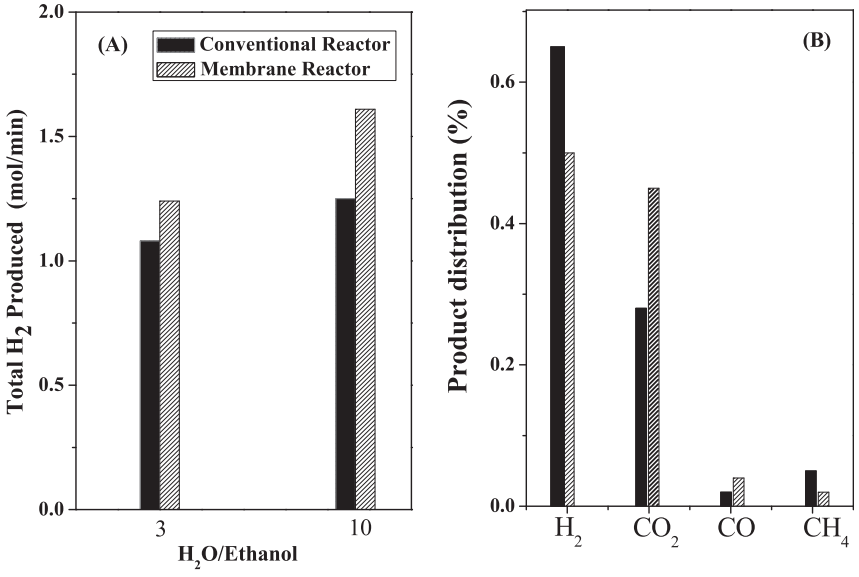

Fig. 8 – Comparison study between reactors: Membrane reactor vs conventional reactor A) Produced H_2, B) Product distribution in the reaction side. Catalyst: Rh/CeO_2. Reaction Conditions: T = 773 K, Ethanol composition = 2.5%, H_2O/Ethanol = 10, W/Q = 0.028 g s/mL.

Tosti et al. [15] studied the SR of ethanol in a membrane reactor, built with a highly hydrogen selective membrane, using Pt and Ni catalysts supported on Al_2O_3 and SiO_2, respectively. They found that both catalysts presented similar activity. Recently, Basile and coworkers [17] compared the activity of two catalysts based on Ni and Co. The authors found that the Ni/ZrO_2 system presented the highest activity but the hydrogen recovery was lower than that obtained with the Co/Al_2O_3. This result was attributed to the higher hydrogen selectivity of the former solid.

The theoretical value of hydrogen produced should be 6 mol for each mole of ethanol reacted. In this work, this value was <6 in all cases. This indicates that in addition to the ethanol reforming reaction, other reactions such as water gas shift, ethanol decomposition, acetaldehyde steam reforming, acetaldehyde decomposition or steam reforming of methane occurs. It is worth noting that in our case no carbon formation was observed for the two catalysts evaluated, which would suggest that the ethanol reaction occurred through dehydrogenation of ethanol to acetaldehyde and not through dehydration of ethanol to ethylene.

Considering that the Rh/CeO_2 catalyst in the MR shows a higher permeated hydrogen/feed ethanol ratio, it was selected to study the set of parameters influencing the membrane reactor performance.

Effect of the steam/ethanol ratio

Fig. 7A shows the effect of the H_2O/Ethanol molar ratio on permeated H_2 employing different SG flow rates with a membrane permeation area of 2.5×10^{-4} m^2. The highest hydrogen permeated flux was obtained under a H_2O/Ethanol = 6 for all SG flow rates, while hydrogen permeated fluxes were lower for the stoichiometric ratio (H_2O/Ethanol = 3). In this case, hydrogen permeation decreases at higher SG flow rate. This behavior could be related to the change in the reaction atmosphere that takes place when hydrogen is extracted from the reactor, promoting the carbon formation and deactivation of the catalyst [40]. The results obtained with a H_2O/Ethanol molar ratio of 10 suggest that part of the water excess dilutes the hydrogen produced in the reaction zone resulting in a lower hydrogen partial pressure difference between both sides of the membrane. Tosti et al. [20] reported that an excess of a limiting reagent increases the reaction conversion in a traditional reactor. However, in a membrane reactor such an excess reduces the partial pressure of the permeating species (hydrogen) and as a consequence, the shift effect of the membrane is depressed.

The results of H_2 recovery as a function of SG flow rate for different H_2O/Ethanol molar ratios are shown in Fig. 7B. The H_2 recovery increases with the SG flow rate for all H_2O/Ethanol ratios. With a H_2O/Ethanol ratio = 6, the H_2 recovery reaches values around 58% with a SG flow rate of 130 mL/min and a membrane permeation area of 2.5×10^{-4} m^2. In our work, it was possible to recover 58% of total hydrogen produced with the additional advantage of producing high purity hydrogen. Basile and coworkers [17] studied the SR of ethanol with a H_2O/Ethanol ratio = 4, at (673 K) and 12 atm using a composite Pd membrane supported on porous stainless steel (Pd/PSS) with a H_2 selectivity close to 90. The authors obtained a hydrogen recovery of 40% under these conditions.

For the SR of ethanol, Gallucci et al. [11] defined the SG ratio as the ratio between the sweep gas flow rate and the ethanol feed flow rate. They reported that the highest increase in the ethanol conversion was observed in the SG ratio range between 1 and 8. Afterwards, the conversion reached a plateau. They remarked that an increase of the SG ratio just makes the hydrogen containing stream in the shell side much diluted without any benefit in terms of reactor performance. In our case, the ethanol conversion was 100% for all reaction conditions used. Then, the effect of the SG ratio on H_2 permeation and recovery was studied. The SG ratio values were varied

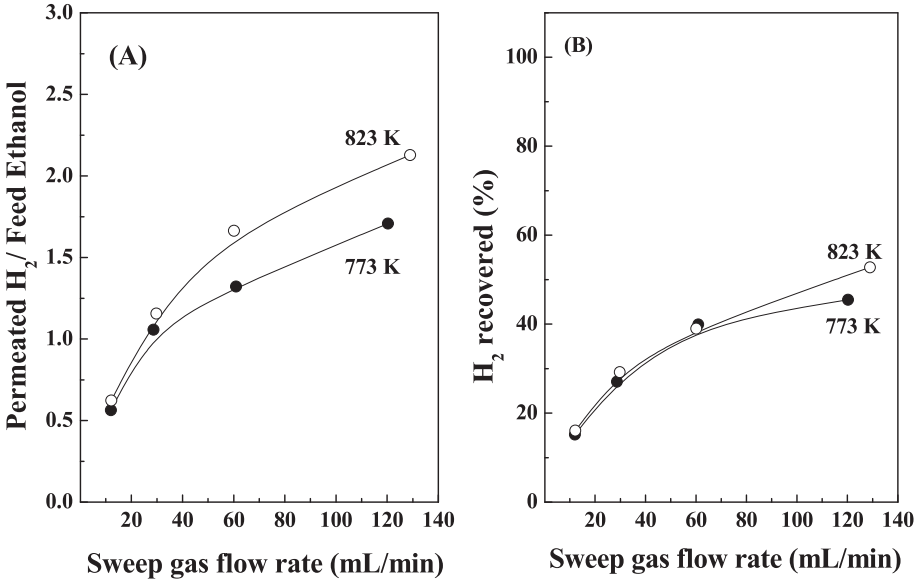

Fig. 9 – Effect of temperature upon the H_2 permeated/ethanol fed ratio (A) and H_2 recovery (B). Catalyst: Rh/CeO_2. Reaction Conditions: H_2O/ethanol = 10.0, Ethanol composition = 2.5%, W/Q = 0.028 g s/mL, Permeation area: 2.5×10^{-4} m^2.

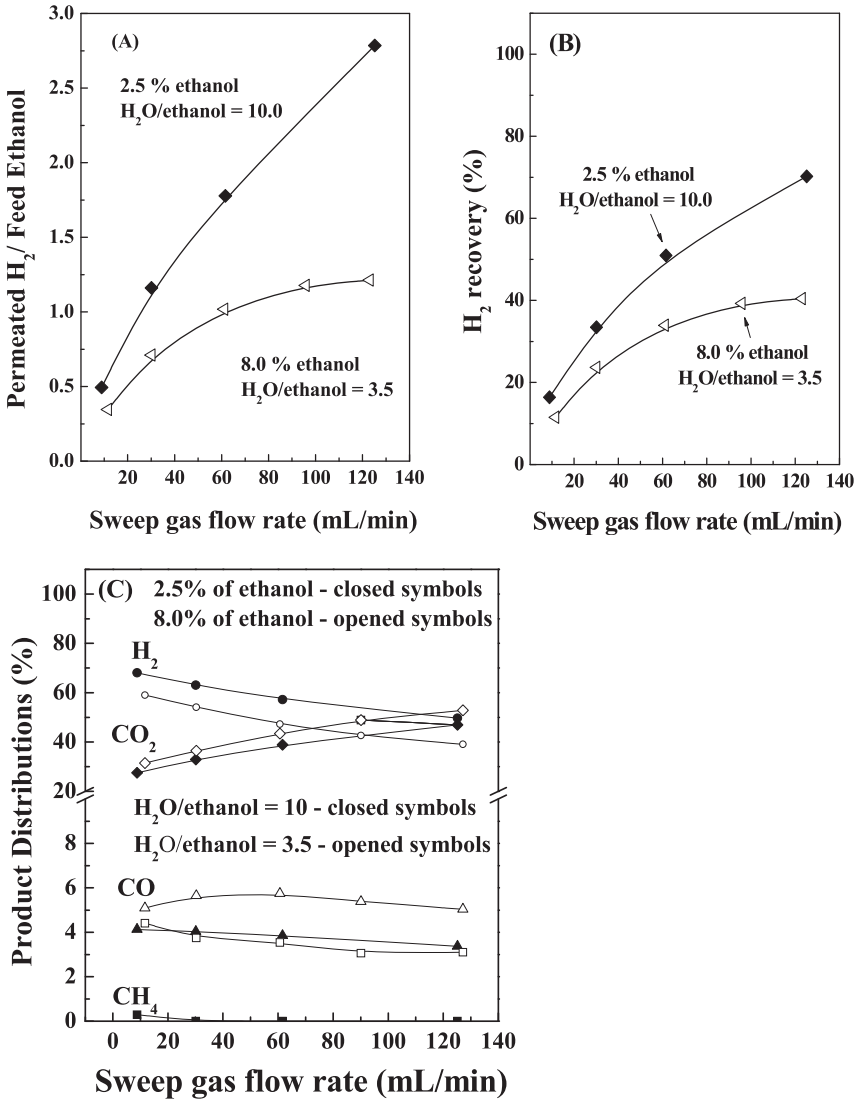

Fig. 10 – Effect of ethanol composition upon the H_2 permeated/ethanol fed ratio (A), H_2 recovery(B) and product distribution (C). Catalyst: Rh/CeO_2. Reaction Conditions: T = 823 K, W/Q = 0.028 g s/mL, Permeation area: 4.0 × 10^{-4} m^2.

between 4.5 (10 mL min^{-1}) and 55 (120 mL min^{-1}). A lower increase was observed when SG ratios higher than 20 were applied.

Comparison between conventional and membrane reactors

Fig. 8 shows the results of the total hydrogen produced (Fig. 8A) and gas composition in the reaction side (Fig. 8B) for the MR and the CR under different H_2O/Ethanol molar ratios. For the MR, the total H_2 produced increased 30% compared to the CR for the H_2O/Ethanol ratio = 10. In both configurations, the ethanol conversion was always 100%. This indicates that the hydrogen producing reactions are favored when a membrane reactor is used. The total H_2 produced for a H_2O/Ethanol ratio = 3 was lower compared with the highest H_2O/Ethanol ratio. Note that the higher H_2 recovery was obtained for the lower H_2O/Ethanol ratio (Fig. 7). This result suggests that when a higher reactant ratio is used, the limiting step could be the hydrogen permeation due to the dilution of hydrogen in the reaction side.

The product distribution in the reaction side for a H_2O/Ethanol molar ratio equal to 10 is shown in Fig. 8B. For the MR, the H_2 concentration in the reaction (retentate) side is lower than the value in the CR. However, due to the H_2 permeation through the membrane, an increase in the total production of hydrogen was observed (Fig. 8A). In addition, the CO_2 concentration increases significantly while the CH_4 decreases in the reaction side (Fig. 8B). It is worth noting that working under the reaction conditions selected in this work (W/Q, T, H_2O/Ethanol ratio) no primary products (acetaldehyde and ethylene) were observed in the reaction side. Oyama and coworkers [21] used membranes with similar permeances but different H_2 selectivity ratios (H_2/CH_4 = 60 and 350). They found that the yield of the primary product (acetaldehyde and ethylene) decreased while the secondary products (H_2, CO_2, CO and CH_4) increased at 623 K

and employing a Co–Na/ZnO catalyst. In our case, only secondary products were obtained in both reactors (CR and MR) which is likely due to the properties of Rh metal. The increase in the total hydrogen (Fig. 8A) and CO_2 production using the membrane reactor would indicate that the overall ethanol reforming reaction is favored under these conditions without the formation of carbon deposits.

Effect of temperature

Fig. 9 shows the results of both H_2 permeated and H_2 recovery as a function of SG flow rate measured at 773 and 823 K. The increase of the permeated flux with temperature is likely due to the highest H_2 permeation through the membrane at higher temperature. A slight difference in the H_2 permeated flux at low SG flow rate is observed. However, at higher SG fluxes the difference is more notorious. This effect can be explained by considering the temperature dependence of the hydrogen permeation through the membrane that can be expressed by an Arrhenius-like equation. The hydrogen transport in thicker palladium membranes takes place through a solution/diffusion mechanism.

Iulianelli and Basile [10] investigated the effect of reaction temperature on the conversion of ethanol in membrane reactors. Taking into account that SR of ethanol is an endothermic reaction, the ethanol conversion is favored by an increase in temperature. In the case of Pd-based MRs, increasing temperature enhanced the hydrogen permeating flux, which shifts the equilibrium of the reaction towards the reaction products, globally increasing the conversion. In our work, the space velocity used allows obtaining an ethanol conversion of 100% at the reaction temperatures employed (773 K and 823 K).

Llorca and coworkers [39] employed a Pd–Rh/CeO_2 catalyst over cordierite monoliths, implemented in-series with a Pd–Ag membrane for hydrogen separation from the monoliths outlet. They also studied the effect of temperature between 823 and 923 K, at complete ethanol conversion. At these temperatures, they observed higher methane conversions assigned to the steam reforming of methane reaction and, consequently, leading to higher hydrogen yields. In addition, an increase in the permeated H_2 flow was observed as temperature increased to 923 K, which was also caused by the temperature dependence of the hydrogen permeation.

Effect of the ethanol composition

The influence of the water to ethanol ratio on the performance of MR has been largely reported in the literature but these studies have not addressed the effect of feed ethanol composition. This work discusses the effect of ethanol composition on H_2 permeation and recovery (Fig. 10). In this case, the water concentration was kept constant and then the H_2O/Ethanol molar ratio varied. In order to increase the hydrogen permeated/ethanol ratio, a permeation area of 4.0×10^{-4} m^2 and a reaction temperature of 823 K were employed. The highest permeated and H_2 recovery were obtained for low ethanol content in the feed (high H_2O/Ethanol ratio). This result is in agreement with the hydrogen production obtained under these conditions (Fig. 10C). The product distribution shows that methane formation is favored under high ethanol concentration, in agreement with the low production of hydrogen. This is also consistent with the increased production of CO, indicating that the ethanol decomposition reaction could be favored at a higher concentration of ethanol.

Effect of the residence time (W/Q)

Fig. 11 shows the performance of the MR at 823 K using two different contact time (W/Q), while the mass of catalyst and the H_2O/Ethanol molar ratio were kept constant. Increasing

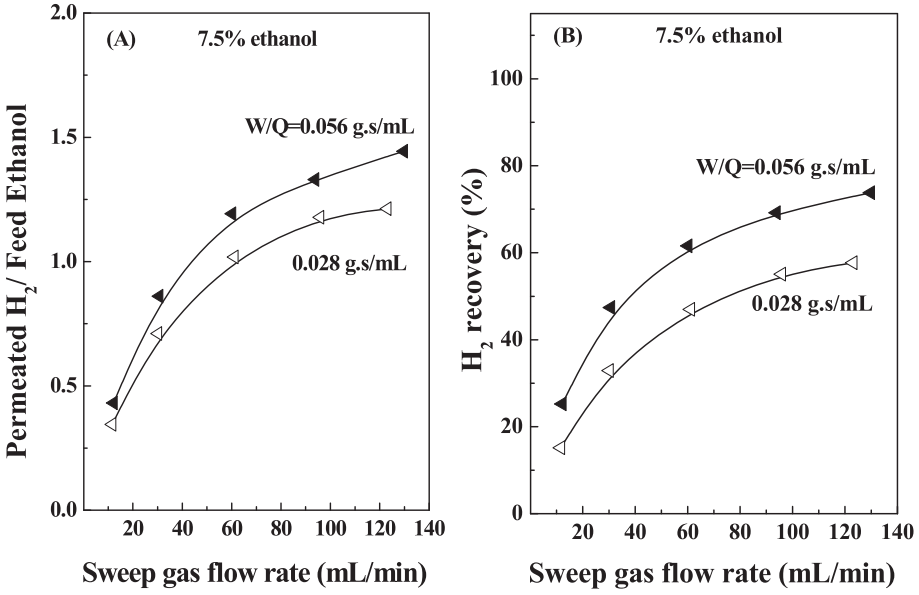

Fig. 11 – Effect of W/Q upon the H_2 permeated/ ethanol fed ratio (A) and H_2 recovery (B). Catalyst: Rh/CeO_2. Reaction Conditions: T = 823 K, H_2O/ethanol = 3.5, Ethanol composition = 7.5%, Permeation area: 4.0×10^{-4} m^2.

W/Q, a higher flux of hydrogen permeated is obtained (Fig. 11A) at all SG flow rates. In addition, the H_2 recovery increased, reaching values at about 72%. Tosti et al. [15] reported that ethanol conversion and hydrogen production decreased when the contact time decreased. The hydrogen yield was strongly dependent on the feed flow rate; the highest values were attained by feeding 5 g h^{-1} of a mixture containing a water/ethanol molar ratio equal to 10. In our work, the ethanol conversion was always 100%. Therefore, the results shown in Fig. 11 can be explained taking into account that for higher W/Q, the formation of secondary products (H_2, CO, CO_2, etc) is favored due to the increase in contact time, causing an increase in the hydrogen partial pressure in the reactor retentate side. Lim et al. [21] studied the effect of space velocity by varying the catalyst amount loaded and the reactant flow rate at 623 K. They found that decreasing the space velocity, the ethanol conversion and the selectivity to CO and CH_4 increased, whereas the selectivity towards CH_3CHO decreased. This result is likely due to the decomposition of acetaldehyde reaction. These results indicated that acetaldehyde is a primary product of ethanol reforming, while CO_2 and CH_4 are secondary products.

Conclusions

This work compared the performance of $Rh/La_2O_3–SiO_2$ and Rh/CeO_2 catalysts for SR of ethanol in a conventional fixed-bed reactor and a membrane reactor. This reactor was built with a self-supported Pd–Ag membrane.

The effect of several operation variables such us sweep gas flow rate, steam to ethanol molar ratio, ethanol concentration, reaction temperature and contact time on H_2 permeation and H_2 recovery was investigated. In all cases, the ethanol conversion was kept at 100%, and the products formed were only H_2, CO_2, CO and CH_4. A higher total hydrogen and CO_2 production was observed in the MR in comparison to the conventional reactor, indicating that the overall ethanol reforming reaction was favored under these conditions without the formation of carbon deposits.

The sweep gas ratio values were varied between 4.5 and 55. A lower increase in H_2 permeation and H_2 recovery was observed when sweep ratios higher than 20 were applied. Both H_2 permeated and H_2 recovery increased when the reaction temperature increased, which was likely due to the highest H_2 permeation through the membrane at higher temperature.

The best results were obtained with a H_2O/Ethanol molar ratio equal to 10 and the highest membrane permeation area of 4×10^{-4} m^2. Under these conditions, the H_2 recovery reached values about 70% with the additional advantage of producing high purity hydrogen.

When Rh-based catalysts were compared, a slight difference in the hydrogen permeated/feed ethanol ratio was observed at higher SG flow rates being higher for Rh supported on CeO_2. For the $Rh/La_2O_3–SiO_2$ catalyst, the concentration of H_2 was lower and the methane concentration slightly increases with the sweep gas flow rate, probably because this catalyst tends to produce more CH_4, lowering the hydrogen produced in the reaction side.

Acknowledgments

The authors wish to acknowledge the financial support received from UNL, ANPCyT, CONICET and CNPq (PROSUL). Thanks are also given to Elsa Grimaldi for the English language editing and to Fernanda Mori for the XPS measurements.

REFERENCES

[1] Hirschenhofer JH, Atauffer DB, Engleman RR, Klent MG. Fuel cell handbook. 4th ed. 1998.
[2] de Lima SM, Colman RC, Jacobs G, Davis BH, Souza KR, de Lima AFF, et al. Hydrogen production from ethanol for PEM fuel cells. An integrated fuel processor comprising ethanol steam reforming and preferential oxidation of CO. Catal Today 2009;146:110–23.
[3] Gallucci F, Fernandez E, Corengia P, van Sint Annaland M. Recent advances on membranes and membrane reactors for hydrogen production. Chem Eng Sci 2013;92:40–66.
[4] Faroldi B, Lombardo EA, Cornaglia LM. Ru/La_2O_3-SiO_2 catalysts for hydrogen production in membrane reactors. Catal Today 2011;172:209–17.
[5] Faroldi B, Bosko ML, Munera J, Lombardo E, Cornaglia L. Comparison of $Ru/La_2O_2CO_3$ performance in two different membrane reactors for hydrogen production. Catal Today 2013;213:135–44.
[6] Carrara C, Roa A, Cornaglia L, Lombardo EA, Mateos-Pedrero C, Ruiz P. Hydrogen production in membrane reactors using Rh catalysts on binary supports. Catal Today 2008;133:334–50.
[7] Mattos LV, Jacobs G, Davis BH, Noronha FB. Production of hydrogen from ethanol: review of reaction mechanism and catalyst deactivation. Chem Rev 2012;112:4094–123.
[8] Haryanto A, Fernando S, Murali N, Adhikari S. Current status of hydrogen production techniques by steam reforming of ethanol. Energy Fuels 2005;19:2098–106.
[9] de la Piscina PR, Homs N. Use of biofuels to produce hydrogen (reformation processes). Chem Soc Rev 2008;37:2459–67.
[10] Iulianelli A, Basile A. Hydrogen production from ethanol via inorganic membrane reactors technology: a review. Catal Sci Technol 2011;1:366–79.
[11] Gallucci F, De Falco M, Tosti S, Marrelli L, Basile A. Ethanol steam reforming in a dense Pd–Ag membrane reactor: a modelling work: comparison with the traditional system. Int J Hydrogen Energy 2008;33(2):644–51.
[12] Gallucci F, van Sint Annaland M, Kuipers JAM. Pure hydrogen production via autothermal reforming of ethanol in a fluidized bed membrane reactor: a simulation study. Int J Hydrogen Energy 2010;35:1659–68.
[13] Gallucci F, De Falco M, Tosti S, Marrelli L, Basile A. Co-current and counter-current configurations for ethanol steam reforming in a dense Pd–Ag membrane reactor. Int J Hydrogen Energy 2008;33(21):6165–71.
[14] Tosti S, Basile A, Borelli R, Borgognoni F, Castelli S, Fabbricino M, et al. Ethanol steam reforming kinetics of a Pd – Ag membrane reactor. Int J Hydrogen Energy 2009;34(11):4747–54.
[15] Tosti S, Basile A, Borgognoni F, Capaldo V, Cordiner S, Di Cavec S, et al. Low temperature ethanol steam reforming in a Pd-Ag membrane reactor: part 1: Ru-based catalyst. J Membr Sci 2008;308:250–7.
[16] Iulianelli A, Basile A. An experimental study on bio-ethanol steam reforming in a catalytic membrane reactor. Part I:

temperature and sweep-gas flow configuration effects. Int J Hydrogen Energy 2010;35:3170–7.
[17] Seelam PK, Liguori S, Iulianelli A, Pinacci P, Calabrò V, Huuhtanen M, et al. Hydrogen production from bio-ethanol steam reforming reaction in a Pd/PSS membrane reactor. Catal Today 2012;193(1):42–8.
[18] Papadias DD, Lee SHD, Ferrandon M, Ahmed S. An analytical and experimental investigation of high-pressure catalytic steam reforming of ethanol in a hydrogen selective membrane reactor. Int J Hydrogen Energy 2010;35(5):2004–17.
[19] Basile A, Pinacci P, Iulianelli A, Broglia M, Drago F, Liguori S, et al. Ethanol steam reforming reaction in a porous stainless steel supported palladium membrane reactor. Int J Hydrogen Energy 2011;36:2029–37.
[20] Tosti S, Fabbricino M, Moriani A, Agatiello G, Scudieri C, Borgognoni F, et al. Pressure effect in ethanol steam reforming via dense Pd-based membranes. J Membr Sci 2011;377:65–74.
[21] Lim H, Gu Y, Oyama ST. Reaction of primary and secondary products in a membrane reactor: studies of ethanol steam reforming with a silica–alumina composite membrane. J Membr Sci 2010;351:149–59.
[22] Lim H, Gu Y, Oyama ST. Studies of the effect of pressure and hydrogen permeance on the ethanol steam reforming reaction with palladium and silica based membranes. J Membr Sci 2012;396:119–27.
[23] Iulianelli A, Liguori S, Longo T, Tosti S, Pinacci P, Basile A. An experimental study on bio-ethanol steam reforming in a catalytic membrane reactor. Part II: reaction pressure, sweep factor and WHSV effects. Int J Hydrogen Energy 2010;35:3159–64.
[24] Tosti S, Zerbo M, Basile A, Calabro V, Borgognon F, Santucci A. Pd-based membrane reactors for producing ultra pure hydrogen: oxidative reforming of bio-ethanol. Int J Hydrogen Energy 2013;38:701–7.
[25] Yun S, Lim H, Ted Oyama S. Experimental and kinetic studies of the ethanol steam reforming reaction equipped with ultrathin Pd and Pd–Cu membranes for improved conversion and hydrogen yield. J Membr Sci 2012;409–410:222–31.
[26] Domok M, Baan K, Kecskes T, Erdohelyi A. Promoting mechanism of potassium in the reforming of ethanol on Pt/Al_2O_3 catalyst. Catal Lett 2008;126:49–57.
[27] Song H, Ozkan US. Changing the oxygen mobility in Co/Ceria catalysts by Ca Incorporation: Implications for ethanol steam reforming. J Phys Chem A 2010;114:3796–801.
[28] Fatsikostas AN, Verykios XE. Reaction network of steam reforming of ethanol over Ni-based catalysts. J Catal 2004;225:439–52.
[29] da Silva AM, de Souza KR, Jacobs G, Graham UM, Davis BH, Mattos LV, et al. Steam and CO_2 reforming of ethanol over Rh/CeO_2 catalyst. Appl Catal B 2011;102:94–109.
[30] Silva FA, Hori CE, Adriana M, Mattos LV, Múnera J, Cornaglia L, et al. Hydrogen production through CO_2 reforming of CH_4 over Pt/$CeZrO_2$/Al_2O_3 catalysts using a Pd – Ag membrane reactor. Catal Today 2012;193(1):64–73.
[31] Zafeiratos S, Nehasil V, Ladas S. X-ray photoelectron spectroscopy study of rhodium particle growth on different alumina surfaces. Surf Sci 1999;433:612–6.
[32] Shyu JZ, Weber WH, Gandhi HS. Surface characterization of alumina-supported ceria. J Phys Chem 1988;92:4964–70.
[33] Noronha FB, Fendley EC, Soares RR, Alvarez WE, Resasco DE. Correlation between catalytic activity and support reducibility in the CO2 reforming of methane over Pt/CexZr1−xO2 catalysts. Chem Eng J 2001;82:21–31.
[34] Miró EE, Ravelli F, Ulla MA, Cornaglia LM, Querini CA. Catalytic combustion of diesel soot on Co, K supported catalysts. Catal Today 1999;53:631–8.
[35] Larachi F, Pierre J, Adnot A, Bernis A. Ce 3d XPS study of composite $Ce_xMn_{1-x}O_{2-y}$ wet oxidation catalysts. Appl Surf Sci 2002;195:236–50.
[36] de Lima SM, da Silva AM, Graham UM, Jacobs G, Davis BH, Mattos LV, et al. Ethanol decomposition and steam reforming of ethanol over $CeZrO_2$ and Pt/$CeZrO_2$ catalyst: reaction mechanism and deactivation. Appl Catal A Gen 2009;352:95–113.
[37] Múnera John F, Irusta S, Cornaglia LM, Lombardo EA, Vargas Cesar D, Schmal M. Kinetic studies of the dry reforming of methane over the Rh/La_2O_3-SiO_2 catalyst. Ind Eng Chem Res 2007;46:7543–9.
[38] Coronel L, Múnera JF, Tarditi A, Moreno MS, Cornaglia L. Hydrogen production by ethanol steam reforming over Rh nanoparticles supported on lanthana/silica systems. Appl Catal B Env 2014;160–161:254–66.
[39] López Eduardo, Divins Nuria J, Llorca Jordi. Hydrogen production from ethanol over Pd–Rh/CeO_2 with a metallic membrane reactor. Catal Today 2012;193:145–50.
[40] Múnera JF, Carrara C, Cornaglia LM, Lombardo EA. Combined oxidation and reforming of methane to produce pure H_2 in a membrane reactor. Chem Eng J 2010;161:204–11.